

Junction area dependent performance of graphene/silicon based self-powered Schottky photodiodes

Mehmet Fidan^a, Özhan Ünverdi^b, Cem Çelebi^{a,*}

^a Quantum Device Laboratory, Department of Physics, Izmir Institute of Technology, 35430, Izmir, Turkey

^b Faculty of Engineering, Department of Electrical and Electronic Engineering, Yaşar University, 35100, Izmir, Turkey



ARTICLE INFO

Article history:

Received 2 February 2021

Received in revised form 3 May 2021

Accepted 12 May 2021

Available online 17 June 2021

Keywords:

Graphene

Schottky junction

Responsivity

Detectivity

Noise equivalent power

Response speed

ABSTRACT

This work reports the impact of junction area on the device performance parameters of Graphene/n-Silicon (Gr/n-Si) based Schottky photodiodes. Herein, three batches of Gr/n-Si photodiode samples were produced based on various sized CVD grown monolayer graphene layers transferred on individual n-Si substrates. The fabricated devices exhibited strong Schottky diode character and had high spectral sensitivity at 905 nm peak wavelength. The optoelectronic measurements showed that the spectral response of Gr/n-Si Schottky photodiodes has a linear dependence on the active junction area. The sample with 20 mm² junction area reached a spectral response of 0.76 AW⁻¹, which is the highest value reported in the literature for self-powered Gr/n-Si Schottky photodiodes without the modification of graphene electrode. In contrast to their spectral responsivities, the response speed of the samples were found to be lowered as a function of the junction area. The experimental results demonstrated that the device performance of Gr/n-Si Schottky photodiodes can be modified simply by changing the size of the graphene electrode on n-Si without need of external doping of graphene layer or engineering Gr/n-Si interface. This study may serve towards the standardization of junction area for the development of high performance Gr/Si based optoelectronic devices such as solar cells and photodetectors operating in between the ultraviolet and near-infrared spectral region.

© 2021 Elsevier B.V. All rights reserved.

1. Introduction

Photodiodes based on graphene/semiconductor heterojunctions have attracted great interest in the years since they exhibit high spectral responsivities and reduced dark currents comparable to those of commercial p-n or p-i-n type photodiodes. It has been shown that a rectifying Schottky junction is created when graphene is interfaced with most of the semiconducting materials like Si, GaAs, GaN and ZnO [1–4]. For example, a Schottky barrier height in an energy range between 0.3–1.0 eV has been identified for the heterojunction of chemical vapor deposition (CVD) grown p-type graphene (Gr) and n-type Si (n-Si) substrate [5–10]. The electric field arising from the built-in potential of around 0.5 – 0.7 V is strong enough to effectively separate the photo-generated charge carriers at the depletion region of Gr/n-Si heterojunction subject to light applied in between ultraviolet and near-infrared spectral region [1,11–13]. Under the influence of light illumination, electrons moved to n-Si and holes injected to graphene electrode give

rise to a measurable photocurrent and an open-circuit voltage in the Gr/n-Si devices even under zero-bias conditions. Therefore, Gr/n-Si heterostructure is utilized as a Schottky photodiode operating in self-powered (photovoltaic) mode which is tempting for solar cells and photo-detection without power consumption.

The device characteristics including the spectral response (R), specific detectivity (D*), noise equivalent power (NEP) and response speed of Gr/n-Si based Schottky junction photodiodes have been studied extensively in earlier works [14–19]. Most of the researchers constructed these type of photodiodes with different device designs for enhancing their photo-response performance. Their photodiode characteristics were found to vary substantially depending on the doping level of Gr layer and/or of n-Si substrate underneath and as well as on the presence/absence of an oxide layer at their interface as shown in Table 1. For example, Lv. et al. demonstrated a photovoltaic type near-infrared photodiode based on the heterojunction of CVD grown monolayer graphene with lightly doped n-Si [15]. Under an illumination of 850 nm wavelength light, R, D* and response time of the device were measured as 29 mA W⁻¹, 3.9 × 10¹¹ Jones, and ~100 μs at zero-bias voltage, respectively. Aydin et al. showed that the maximum R of Gr/n-Si Schottky photodiodes at 850 nm peak wavelength can be increased from 0.24

* Corresponding author.

E-mail address: cemcelebi@iyte.edu.tr (C. Çelebi).

Table 1

The device characteristics of the near-infrared Schottky photodiodes based on Gr/n-Si heterojunction studied in literature, at room temperature.

Device structure	Response λ (nm)	R (AW^{-1})	D^* (Jones)	NEP ($pWHz^{-1/2}$)	t_r / t_d (μs)	Ref.
Gr/n-Si	850	0.029	3.9×10^{11}	–	93 / 110	[15]
Gr/n-Si	850	0.24	1.9×10^{10}	0.20	–	[17]
P3HT Gr/n-Si	850	0.78	2.6×10^{10}	0.14	–	[17]
Gr/n-Si	890	0.73	4.2×10^{12}	0.075	320 / 750	[14]
Gr/SiO ₂ /n-Si	890	0.73	4.1×10^{13}	0.0078	320 / 750	[14]

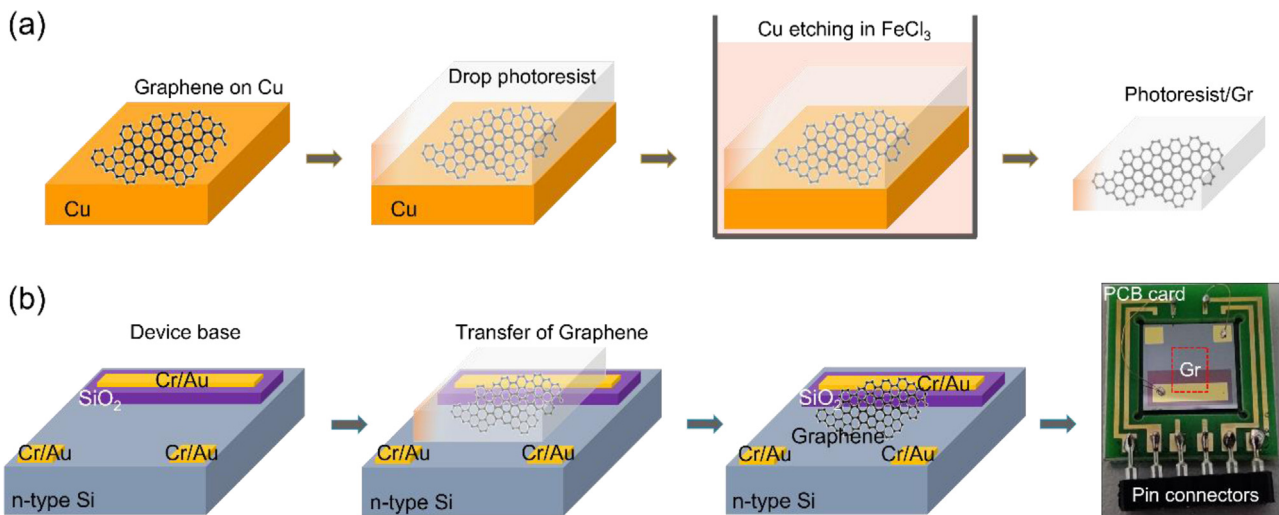


Fig. 1. (a) Schematic illustration of CVD graphene growth on Cu foil and its transfer preparation onto Si substrate, (b) SiO₂ and Cr/Au deposition onto Si substrate, followed by transferring of graphene and Gr/n-Si structure mounted on PCB card.

AW^{-1} to $0.78 AW^{-1}$ when Gr electrode is coated with P3HT polymer molecules [17]. In a subsequent work, Li et al. reported that D^* and NEP values of Gr/n-Si Schottky junction photodiodes can be improved by an order of magnitude with a thin SiO₂ layer at the interface between Gr electrode and n-Si substrate due to strongly reduced dark current [14].

Different from previous studies reported in the literature, we systematically investigated the impact of junction area on the above-mentioned device parameters of self-powered Gr/n-Si photodiodes. For the experiments, a set of Gr/n-Si heterojunction devices was fabricated, in which a monolayer CVD grown graphene was employed as Schottky electrode and acted as the active region when interfaced with n-Si substrate. The junction area is changed by transferring graphene with different dimensions (e.g., $4 mm^2$, $12 mm^2$ and $20 mm^2$) on three individual n-Si substrates. The electrical characteristics of all the samples displayed excellent rectification behavior. Wavelength resolved photocurrent spectroscopy measurements showed that the maximum spectral response of the photodiodes appears at $905 nm$ peak wavelength and increases linearly from $0.16 AW^{-1}$ to $0.76 AW^{-1}$ as the junction area is increased from $4 mm^2$ to $20 mm^2$. Compared to the one with $4 mm^2$ sized graphene electrode, the photodiode with $20 mm^2$ graphene exhibited lower response speed under the influence of $905 nm$ wavelength light pulsed with $5 kHz$ frequency.

2. Experimental details

For the graphene growth process by CVD technique, high purity Copper (Cu) foils ($25 \mu m$ thick, Alfa Aesar) were cut into pieces of different sizes in order to fabricate Gr/n-Si Schottky diodes with various junction areas. Then the Cu foils placed on a quartz slide was loaded into the tube furnace of CVD system at atmospheric pressure. Subsequently, the chamber was pumped down to its base vacuum level. The Cu foils inside the quartz tube was heated up

to $1000 ^\circ C$ under the flow of H₂ (20 sccm) and Ar (1000 sccm) gas mixture. The samples were annealed for 1 h. under the same temperature and gas flow rates. This provides both removing of the native oxide layer on the Cu foil and forming of (111) oriented grain boundaries. Following the annealing process, CH₄ (10 sccm) gas was delivered into the tube furnace for 2 min. in order to grow the graphene layer on Cu foils. Finally, the tube was left for cooling down to room temperature under gas flows of H₂ (20 sccm) and Ar (1000 sccm). As the supporting layer Microposit S1318 Photoresist (PR) was drop casted on the Gr/Cu and the stack was annealed at $70 ^\circ C$ overnight in an oven. The Cu foil at the bottom was fully etched using Iron Chloride (FeCl₃) solution to get suspended PR/Gr bilayer. After etching of possible FeCl₃ residues in H₂O:HCl (3:1) solution, the PR/graphene became ready for transfer process (see Fig. 1(a)).

A commercial Si wafer (n-type, resistivity of $\rho = 1-5 \Omega.cm$) was used as the substrate for Gr/n-Si Schottky junction photodiode. The wafer was diced into $10 mm \times 10 mm$ square pieces and was ultrasonically cleaned for 10 min. in acetone, isopropanol (IPA) and deionized (DI) water, respectively. The native oxide on the substrates was etched away by 6 % diluted hydrofluoric acid (HF). This is an important process for ensuring good electrical contact on Si, before the deposition of Cr/Au metallic contact pads and graphene transfer process. As seen in Fig. 1(b), 400 nm thick SiO₂ dielectric layer is evaporated to cover a portion of the surface of n-type Si substrate. For conducting two-terminal I-V measurements, Cr/Au ($4 nm/80 nm$) metal contact pads were deposited both on the n-Si side and on the SiO₂ covered side of the substrate by a thermal evaporation system. Necessary for the graphene transfer onto fabricated device base, the PR/Gr was annealed at a temperature of $100 ^\circ C$ for 5 min. in order to provide better adhesion of the graphene layer on the surface of n-Si substrate. One end of the graphene lies on the n-Si surface without touching the metal electrodes deposited on the n-Si and the other end is placed on the Cr/Au pad which was already deposited on the SiO₂ layer. After the transfer of graphene elec-

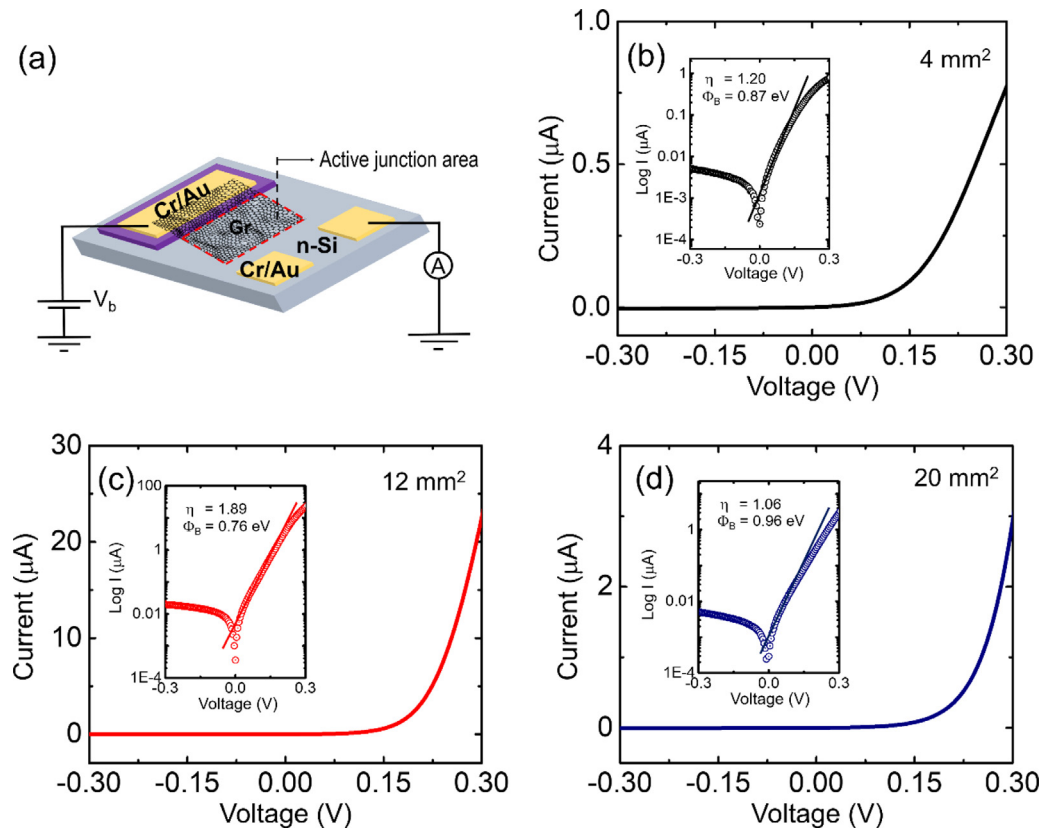


Fig. 2. (a) Schematic illustration of the fabricated Gr/n-Si photodiode. The dark I-V graphs of the Gr/n-Si photodiodes depending on junction areas: b) 4 mm^2 , c) 12 mm^2 and d) 20 mm^2 . Inset shows the dark I-V measurements of the devices on a semi-logarithmic scale, which was used to extract the ideality factor and the barrier height of the diodes.

trode, the supporting PR layer was removed by acetone, followed by rinsing with IPA and DI water, respectively. For two-terminal I-V measurements, $80 \mu\text{m}$ thick Cu wires were bonded both on the Cu plated paths of a PCB card and Cr/Au contact pads by means of a lab-built wire bonder.

The electric and optoelectronic characterizations of the fabricated Gr/n-Si devices were done using Keithley's Source-Meter, Picoammeter and Nanovoltmeter in a unit equipped with a quartz tungsten halogen lamp (Osram, 275 W) light source, a high resolution monochromator (Newport, Oriel Cornerstone), Ocean Optics flame spectrometer and a commercial Si-photodetector (FDS10 × 10, Thorlabs). The I-V measurements were carried out at room temperature in dark and under light illumination of 905 nm wavelength. The irradiation wavelength is specifically selected to be 905 nm since it corresponds to the maximum spectral response of our fabricated Gr/n-Si photodiodes. Power dependent I-V measurements were performed by 905 nm illumination with different light power densities. In addition, time-resolved photocurrent behavior of our devices was also examined using a LED driver with pulse modulation at 905 nm light.

3. Results and discussion

A schematic of the fabricated Gr/n-Si Schottky photodiodes is shown in Fig. 2(a). The junction area pointed out in Fig. 2(a) corresponds to the size of the graphene electrode making direct contact with the n-Si side of the device structure. Firstly, we investigated the dark I-V characteristic of the photodiodes with three different junction areas such as 4 mm^2 , 12 mm^2 and 20 mm^2 . From the obtained I-V measurements the dark current (I_d) of all the devices were extracted as $\sim 0.3 \text{ nA}$. As seen in Fig. 2(b-d), the I-V measure-

ments of the samples displayed typical rectifying Schottky junction behaviour which is in good agreement with the thermionic emission (TE) model [20] given as,

$$I = I_0 \left[\exp \left(\frac{qV}{\eta kT} \right) - 1 \right] \quad (1)$$

where I_0 is the reverse saturation current which is written as,

$$I_0 = AA^* T^2 \exp \left(-\frac{q\Phi_B}{kT} \right) \quad (2)$$

where A is the junction area (0.04 cm^2 , 0.12 cm^2 and 0.2 cm^2 for our Gr/n-Si samples, respectively), A^* is the effective Richardson constant ($112 \text{ A/cm}^2 \text{ K}^2$ for n-Si), T is the temperature (300 K), Φ_B is the Schottky barrier height, k is the Boltzmann constant, q is the elementary charge and η is the ideality factor.

From the I-V data the I_0 values were determined to be 0.75×10^{-8} , 2.61×10^{-8} and 0.78×10^{-8} for the photodiodes with junction area of 4 mm^2 , 12 mm^2 and 20 mm^2 , respectively. From the linear forward-bias region of the $\ln(I)$ -V plot shown at the inset of Fig. 2(b-d), the Schottky diode parameters η and Φ_B for our devices were extracted by using the method developed by Cheung et al. [21]. For the junction areas of 4 mm^2 , 12 mm^2 and 20 mm^2 , the η of our devices were found to be 1.20, 1.89 and 1.06, respectively. By means of the corresponding η values, zero-bias Φ_B of the devices in dark were deduced as 0.87 eV, 0.76 eV and 0.96 eV, respectively. It should be mentioned that these diode parameters are consistent with the previously reported η and Φ_B parameters for the heterojunction of monolayer CVD graphene with n-Si substrate [8,12,18]. The variation in η and Φ_B may originate from the degree of unintentional hole doping of graphene electrode due to the chemicals used in the growth and transfer processes and/or from the inhomogeneities at the Gr/n-Si inter-

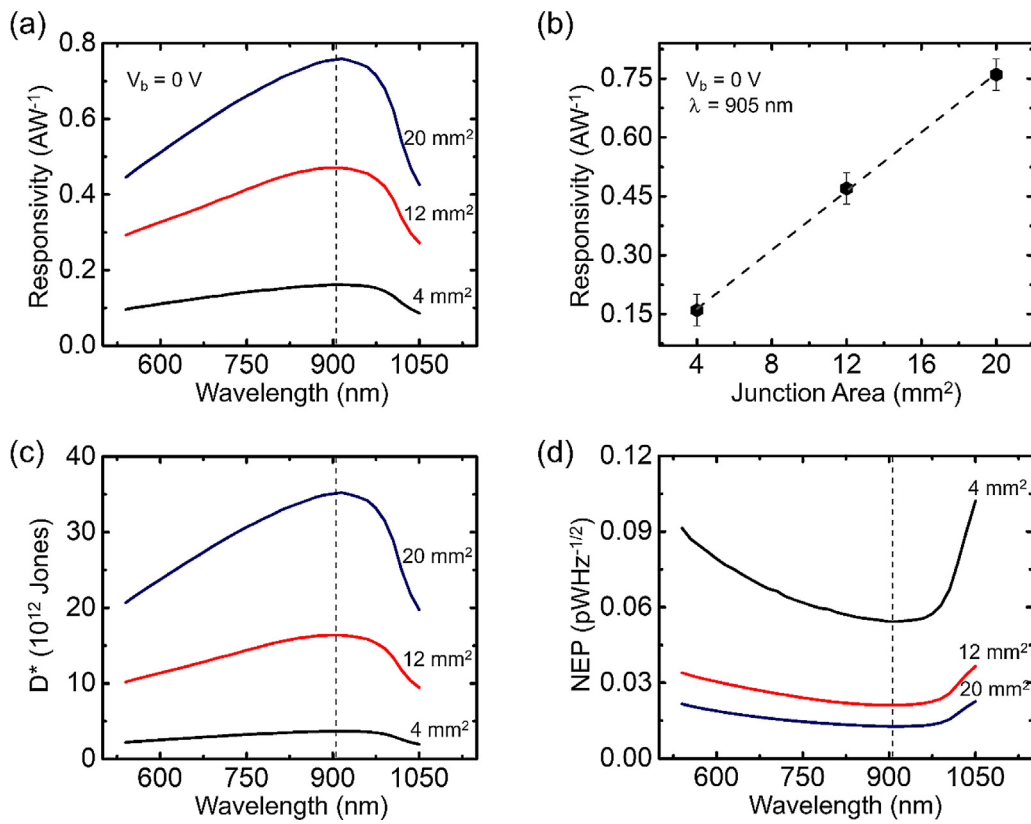


Fig. 3. (a) Responsivity vs. wavelength of the Gr/n-Si devices based on different junction areas at zero-bias voltage. (b) Responsivity of the devices at the peak wavelength of 905 nm at $V_b = 0$ V. (c) D^* and (d) NEP of the fabricated Gr/n-Si photodiodes as a function of wavelength.

face. For example, impurities and defects modify graphene's work function by shifting its Fermi level relative to its charge neutrality point and therefore changes the magnitude of η and ϕ_B in Gr/n-Si heterojunction.

The spectral response (R) is one of the most important device parameters of a photodiode and is defined as the ratio of generated photocurrent (I_{pc}) to the incident light power (P) at a certain wavelength. Zero-bias R of the samples with different junction areas were compared in Fig. 3(a) for the incident light wavelength range between 540 and 1050 nm. In all the measurements, the maximum R appeared at a peak wavelength of 905 nm and exhibited a downward trend towards a cutoff wavelength of 1050 nm due to the band edge of n-Si substrate. The measurements showed that the R parameter of the Gr/n-Si Schottky photodiode has an excellent linear dependence on the junction area as displayed in Fig. 3(b). In our device design the junction area is defined as the photoactive region where the graphene electrode is in direct contact with the underlying Si substrate. Therefore, the dimension of the junction area is determined only by the size of the graphene electrode itself. The large lateral dimensions of the graphene electrode (or the size of junction area) lead to greater depletion region length of the junction. This promotes the vertical electric field across the Gr/n-Si heterojunction and enhances the effective separation/collection of photo-generated charge carriers at the depletion region. Because of enhanced charge separation and collection, the photocurrent and thus the spectral response of our photodiode increase as a function of the size of graphene electrode. The maximum R of 0.76 AW^{-1} was achieved for the device with a junction area of 20 mm^2 . This is the highest R value measured for a self-powered Gr/n-Si Schottky photodiode presented in the literature. Based on the measured R values, we also calculated the specific detectivity (D^*) and noise equivalent power (NEP) parameters of our samples. Here, D^* is defined as the weakest level of light detected by

a photodiode having a junction area of 1 cm^2 and is determined by [17,22],

$$D^* = \frac{A^{1/2} R}{\sqrt{2qI_d}} \quad (3)$$

and NEP is the incident power required to obtain a signal-to-noise ratio of 1 at a bandwidth of 1 Hz and is calculated by [14,17],

$$\text{NEP} = \frac{A^{1/2}}{D} \quad (4)$$

D^* and NEP of our samples were calculated using Eqs. 3 and 4, respectively and the obtained results were displayed as a function of wavelength in Fig. 3(c-d). In agreement with the corresponding R values, the maximum D^* and minimum NEP values were found at 905 nm peak wavelength. With $D^* = 3.5 \times 10^{13} \text{ Jones}$ and $\text{NEP} = 0.013 \text{ pWHz}^{-1/2}$, the sample having a junction area of 20 mm^2 was determined to be the most sensitive one among other samples with smaller junction areas. These obtained results clearly showed that the detection limit of a Gr/n-Si photodiode can be improved simply by increasing its junction area without need of either external doping of the graphene electrode or interface modification of the Gr/n-Si heterojunction.

The variation in the I-V characteristics of our samples illuminated with different light power were displayed in the semi-logarithmic scale in Fig. 4(a-c). All samples exhibit a clear photovoltaic activity under light illumination. In detail, semi-logarithmic scale I-V characteristics of our devices under the illumination of 905 nm wavelength light with $10 \mu\text{W}$ power is shown in Fig. 4(d). For each of the I-V curves, the voltage read at the minimum current and the current at zero-bias correspond to open-circuit voltage (V_{oc}) and short-circuit current (I_{sc}), respectively. The variation in V_{oc} and I_{sc} for each of the sample was plotted

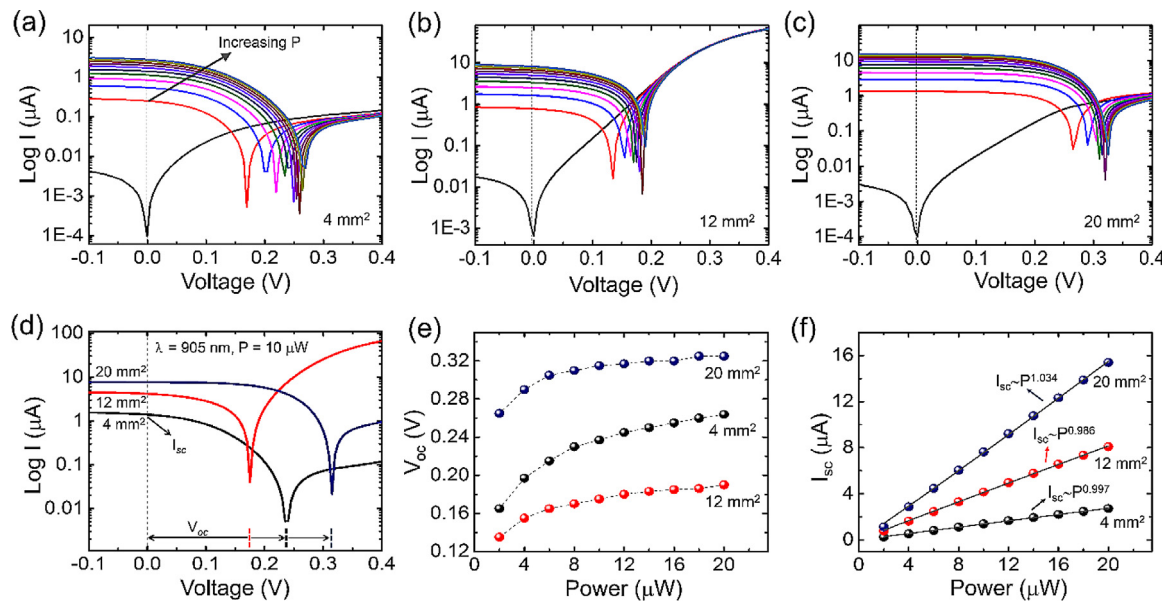


Fig. 4. (a-c) I-V curves at dark and under the irradiation with light power (P) changing from 2 μW to 20 μW . (d) Semi-logarithmic scale I-V characteristics of the devices under a constant light power of 10 μW at 905 nm. (e) V_{oc} and (f) I_{sc} of the fabricated Gr/n-Si photodiodes exposed to 905 nm wavelength light with different power densities. The curves in (f) are fitted by the power law.

in Fig. 4(e-f) as a function of the incident light power. As seen in Fig. 4(e) and (f) although I_{sc} exhibits a clear linear response to the incident light, V_{oc} increases nonlinearly and converges to different saturation levels depending on the junction area as the incident light power exceeds 20 μW . Fitting the plots in Fig. 4(f) with power law of $I_{\text{sc}} \sim P^\theta$, we extracted the factor θ determining the efficiency of photo-generated charges to incident light power. Linear increase of I_{sc} with the light power (where $0.98 \leq \theta \leq 1.03$) confirms that the photocurrent in all the samples is solely determined by the amount of photo-generated charge carriers. The nonlinear variation of V_{oc} with incident light power is typical for Gr/n-Si Schottky photodiodes and can be explained in terms of the quasi-Fermi level transport model including surface recombination mechanism [22,23]. Consistent with the maximum R values, the measured I_{sc} had a linear dependence on the junction area. However, such a trend was not observed for the variation in V_{oc} values. As explained by the quasi-Fermi level transport model, V_{oc} generated in a heterojunction device is strongly governed by the magnitude of Φ_B . Therefore, the inconsistent change of V_{oc} with increasing junction area shown in Fig. 4(e) can be directly associated with the difference in Φ_B of the devices discussed previously.

In order to determine the response speed and 3-dB bandwidth (B_w) of our samples, we conducted time-resolved photocurrent measurements using the experimental set-up illustrated in Fig. 5(a). For the measurements, a 940 nm wavelength collimated LED light source with a broad full width half maximum and a 905 nm laser line bandpass filter are used. The measurements were done for zero-bias condition and the photocurrent data were recorded under 905 nm wavelength light pulsed at 5 kHz frequency. The output photocurrent signal was converted to voltage with a transimpedance amplifier and then measured by an oscilloscope.

Time-resolved photocurrent measurements, which were repeated over several on/off switching cycles within 1.0 ms. total time, showed that all the devices have excellent photocurrent reversibility and stability as seen in Fig. 5(b). Rise time (t_r) and decay time (t_d) of each of the samples were determined from single pulse response measurements. Here t_r is defined as the range that the photocurrent rises from 10 to 90 % of its maximum and t_d is defined similarly. Based on the obtained t_r and t_d values shown

in Fig. 5(c-e), we found that the response speed of our Gr/n-Si Schottky photodiodes decreases as the junction area increases. This is likely caused by the increased number of interface defects for larger junction area, which can act as carrier trapping centers. The slow release of trapped charge carriers results in a long decay edge. This phenomenon is more evident especially at low temperatures because of relatively low trapping energy levels [15]. Rise time and 3-dB B_w are two closely-related parameters used to describe the limit of a circuit's capability to respond to abrupt changes in an input signal. The 3-dB B_w is related to the RC constant of the circuit and determines the operational speed of a photodetector [24]. Using the relation $B_w = 0.35/t_r$ we also estimated the 3-dB B_w of the samples with 4, 12 and 20 mm^2 junction areas as 55, 31 and 22 kHz, respectively. Considering the large junction area and relatively low conductivity of the graphene electrode, it is expected that the response speed of Gr/n-Si photodiodes can be remarkably improved by further optimizing the device design.

The performance parameters of Gr/n-Si photodiodes obtained in this work are compared in Table 2. Depending on the increasing junction area, the photodiode parameters including R, D* and NEP are seemed to be improved. Compared to previously reported Gr/n-Si photodiodes [14–17], our device with the junction area of 20 mm^2 displayed excellent R, D* and NEP values which are 0.76 AW^{-1} , 3.5×10^{13} Jones and 0.013 $\text{pWHz}^{-1/2}$, respectively. However, contrary to the improvement in such photodiode parameters, the device exhibited lower response speed due to larger junction area.

4. Conclusion

To conclude, the effect of junction area on the device characteristics of Gr/n-Si Schottky photodiodes is investigated. A set of photovoltaic type photodiode samples with different junction areas was fabricated by transferring monolayer CVD grown graphene on n-Si substrate. The devices exhibiting rectification behavior have been examined in terms of their spectral response, specific detectivity, noise equivalent power and response speed under self-powered condition. The measurements showed that, in contrast to their response speed, the spectral response of Gr/n-Si based photodiodes increases linearly as a function

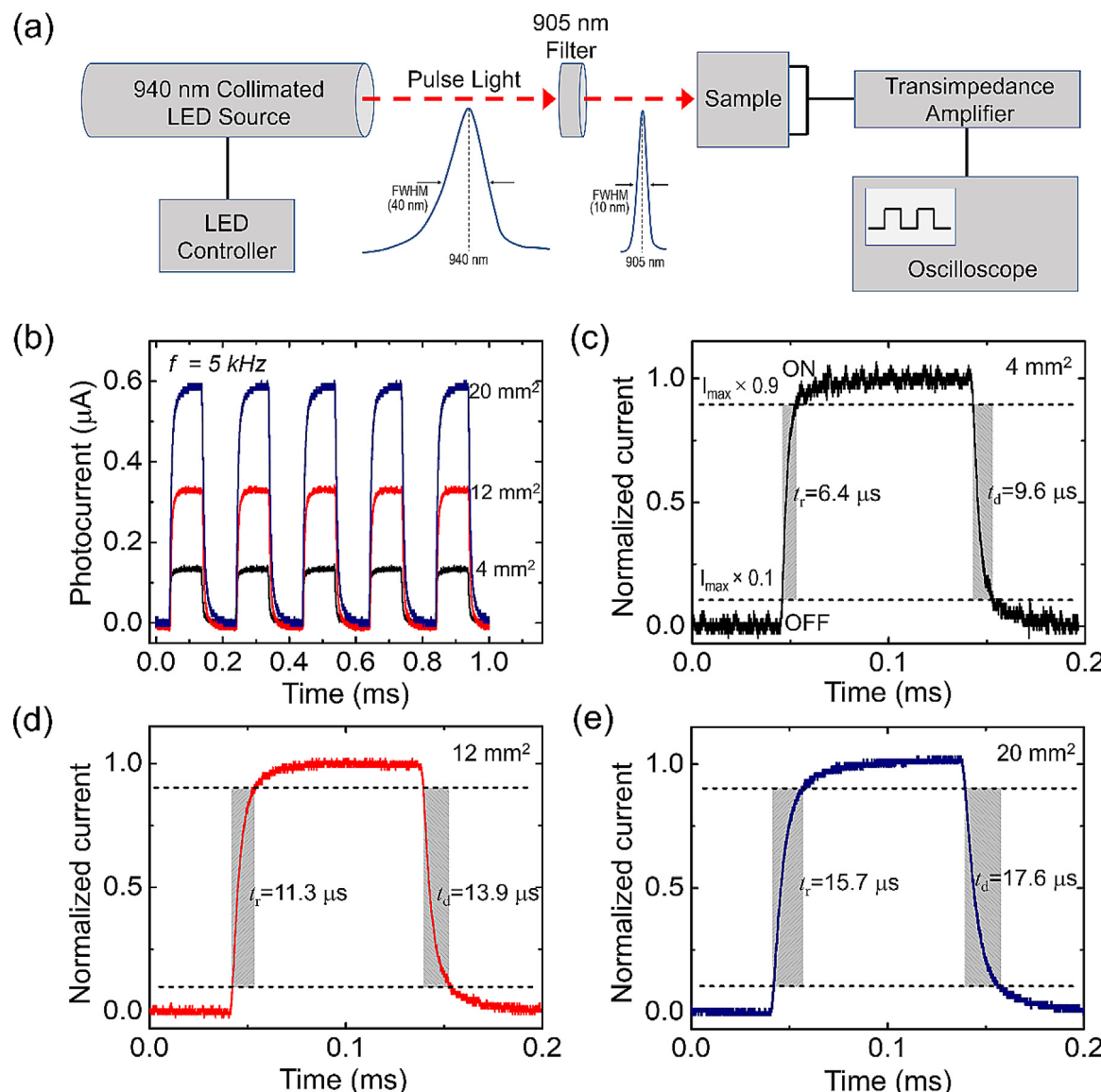


Fig. 5. (a) Schematic diagram of the time-resolved photocurrent measurement system. (b) Time-resolved photocurrent spectrum of the Gr/n-Si photodiodes under fast varied light illumination (905 nm, $\sim 1 \mu\text{W}$) with a light switching frequency of 5 kHz at zero-bias voltage. The 0.2 ms one cycle time-resolved photocurrent spectrum of the Gr/n-Si photodiodes under 905 nm wavelength at zero-bias voltage; depending on junction areas (c) 4 mm^2 , (d) 12 mm^2 and (e) 20 mm^2 . The measured photocurrents were normalized with the maximum values.

Table 2

The performance of the fabricated Gr/n-Si photodiodes under 905 nm wavelength light at 0 V bias.

Junction Area (mm^2)	$R (\text{AW}^{-1})$	$I_d (\text{nA})$	$D^* (\text{Jones})$	$\text{NEP}(\text{pWHz}^{-1/2})$	$t_r (\mu\text{s})$	$t_d (\mu\text{s})$
4	0.16	0.24	0.37×10^{13}	0.055	6.4	9.6
12	0.47	0.31	1.64×10^{13}	0.021	11.3	13.9
20	0.76	0.29	3.53×10^{13}	0.013	15.7	17.6

of the junction area. A maximum spectral response of 0.76 AW^{-1} is achieved at 905 nm peak wavelength for 20 mm^2 junction area which is the highest value reported in the literature for Gr/n-Si based Schottky photodiodes operating under zero-bias condition. The obtained experimental findings suggest that the photo-sensitivity of these type of photodiodes can be improved simply by increasing their junction area without need of either external doping of the graphene electrode or interface modification of the Gr/n-Si heterojunction. This work is expected to provide useful information for the integration of large area graphene in semiconductor based optoelectronic device technology.

Funding

Funding was received for this work.

All of the sources of funding for the work described in this publication are acknowledged below:

Yaşar University, Izmir, Turkey.

Intellectual property

The authors confirm that we have given due consideration to the protection of intellectual property associated with this work and

that there are no impediments to publication, including the timing of publication, with respect to intellectual property. In so doing we confirm that we have followed the regulations of our institutions concerning intellectual property.

Authorship

All listed authors meet the ICMJE criteria. 'We attest that all authors contributed significantly to the creation of this manuscript, each having fulfilled criteria as established by the ICMJE.'

The authors confirm that the manuscript has been read and approved by all named authors.

The authors confirm that the order of authors listed in the manuscript has been approved by all named authors.

Declaration of Competing Interest

No conflict of interest exists.

The authors wish to confirm that there are no known conflicts of interest associated with this publication and there has been no significant financial support for this work that could have influenced its outcome.

Acknowledgements

The authors would like to thank Center for Materials Research at Izmir Institute of Technology and Sparks Electronics Ltd. in Turkey for their support in device fabrication processes. This work is supported as part of the Project No. BAP089 that has been approved by Yaşar University Project Evaluation Commission (PEC).

References

- [1] C.C. Chen, M. Aykol, C.C. Chang, A.F.J. Levi, S.B. Cronin, Graphene-silicon Schottky diodes, *Nano Lett.* 11 (2011) 1863–1867.
- [2] D. Tomer, S. Rajput, L.J. Hudy, C.H. Li, L. Li, Inhomogeneity in barrier height at graphene/Si (GaAs) Schottky junctions, *Nanotechnology* 26 (2015), 215702.
- [3] A.K. Ranade, R.D. Mahavanshi, P. Desai, M. Kato, M. Tanemura, G. Kalita, Ultraviolet light induced electrical hysteresis effect in graphene-GaN heterojunction, *Appl. Phys. Lett.* 114 (2019), 151102.
- [4] F. Qin, C. Xu, G. Zhu, F. Chen, R. Wang, J. Lu, D. You, X. Wang, W. Zhang, J. Zhao, Brightness improvement in a graphene inserted GaN/ZnO heterojunction light emitting diode, *J. Phys. D Appl. Phys.* 52 (2019), 395104.
- [5] F. Liu, S. Kar, Quantum carrier reinvestment-induced ultrahigh and broadband photocurrent responses in graphene-silicon junctions, *ACS Nano* 8 (2014) 10270–10279.
- [6] D. Sinha, J.U. Lee, Ideal graphene/silicon schottky junction diodes, *Nano Lett.* 14 (2014) 4660–4664.
- [7] T. Zhang, M.B. Nix, B.Y. Yoo, M.A. Deshusses, N.V. Myung, Electrochemically functionalized single-walled carbon nanotube gas sensor, *Electroanalysis*. 18 (2006) 1153–1158.
- [8] H.Y. Kim, K. Lee, N. McEvoy, C. Yim, G.S. Duesberg, Chemically modulated graphene diodes, *Nano Lett.* 13 (2013) 2182–2188.
- [9] S. Parui, R. Ruiter, P.J. Zomer, M. Wojtaszek, B.J. Van Wees, T. Banerjee, Temperature dependent transport characteristics of graphene/n-Si diodes, *J. Appl. Phys.* 116 (2014), 244505.
- [10] Y. Wang, S. Yang, A. Ballesio, M. Parmeggiani, A. Verna, M. Cocuzza, C.F. Pirri, S.L. Marasso, The fabrication of Schottky photodiode by monolayer graphene direct-transfer-on-silicon, *J. Appl. Phys.* 128 (2020), 014501.
- [11] T. Yu, F. Wang, Y. Xu, L. Ma, X. Pi, D. Yang, Graphene coupled with silicon quantum dots for high-performance bulk-silicon-Based schottky-junction photodetectors, *Adv. Mater.* 28 (2016) 4912–4919.
- [12] S. Tongay, M. Lemaitre, X. Miao, B. Gila, B.R. Appleton, A.F. Hebard, Rectification at graphene-semiconductor interfaces: zero-gap semiconductor-based diodes, *Phys. Rev. X* 2 (2012), 011002.
- [13] D. Periyangounder, P. Gnanasekar, P. Varadhan, J.H. He, J. Kulandaivel, High performance, self-powered photodetectors based on a graphene/silicon Schottky junction diode, *J. Mater. Chem. C*. 6 (2018) 9545.
- [14] X. Li, M. Zhu, M. Du, Z. Lv, L. Zhang, Y. Li, Y. Yang, T. Yang, X. Li, K. Wang, H. Zhu, Y. Fang, High detectivity graphene-silicon heterojunction photodetector, *Small* 12 (2016) 595–601.
- [15] P. Lv, X. Zhang, X. Zhang, W. Deng, J. Jie, High-sensitivity and fast-response graphene/crystalline silicon schottky junction-based near-IR photodetectors, *IEEE Electron Device Lett.* 34 (2013) 1337–1339.
- [16] X. An, F. Liu, Y.J. Jung, S. Kar, Tunable graphene-silicon heterojunctions for ultrasensitive photodetection, *Nano Lett.* 13 (2013) 909–916.
- [17] H. Aydin, S.B. Kalkan, C. Varlikli, C. Çelebi, P3HT-graphene bilayer electrode for Schottky junction photodetectors, *Nanotechnology* 29 (2018), 145502.
- [18] Y. Wang, S. Yang, D.R. Lambada, S. Shafique, A graphene-silicon Schottky photodetector with graphene oxide interlayer, *Sens. Actuators Phys. A* 314 (2020), 112232.
- [19] C. Wang, Y. Dong, Z. Lu, S. Chen, K. Xu, Y. Ma, G. Xu, X. Zhao, Y. Yu, High responsivity and high-speed 1.55 μm infrared photodetector from self-powered graphene/Si heterojunction, *Sens. Actuators Phys. A* 291 (2019) 87–92.
- [20] S. Sze, *Microelectronics J*, in: *Physics of Semiconductor Devices*, 2nd edition, 1981.
- [21] S.K. Cheung, N.W. Cheung, Extraction of Schottky diode parameters from forward current-voltage characteristics, *Appl. Phys. Lett.* 49 (1986) 85.
- [22] X. Wan, Y. Xu, H. Guo, K. Shehzad, A. Ali, Y. Liu, J. Yang, D. Dai, C. Te Lin, L. Liu, H.C. Cheng, F. Wang, X. Wang, H. Lu, W. Hu, X. Pi, Y. Dan, J. Luo, T. Hasan, X. Duan, X. Li, J. Xu, D. Yang, T. Ren, B. Yu, A self-powered high-performance graphene/silicon ultraviolet photodetector with ultra-shallow junction: breaking the limit of silicon? *Npj 2D Mater. Appl.* 1 (2017) 4.
- [23] L.J.A. Koster, V.D. Mihailescu, R. Ramaker, P.W.M. Blom, Light intensity dependence of open-circuit voltage of polymer:fullerene solar cells, *Appl. Phys. Lett.* 86 (2005), 123509.
- [24] Z. Lu, Y. Xu, Y. Yu, K. Xu, J. Mao, G. Xu, Y. Ma, D. Wu, J. Jie, Ultrahigh speed and broadband few-layer MoTe₂/Si 2D–3D heterojunction-based photodiodes fabricated by pulsed laser deposition, *Adv. Funct. Mater.* 30 (2020), 1907951.

Biographies

Mehmet Fidan received his MSc degree in Physics department from Izmir Institute of Technology (IZTECH), Turkey in 2014. He is pursuing for his pH.D. under the supervision of Assoc. Prof. Dr. Cem Çelebi at the Quantum Device Laboratory (QDL) in Physics department of the same institute. His main research interests include Graphene synthesis and Graphene/Semiconductor heterojunction devices.

Özhan Ünverdi received his pH.D. in 2005 from Physics Department of Loughborough University in UK. He is currently working as Assistant Professor in Electric-Electronics Engineering Department of Yaşar University. His main research areas are low-dimensional systems, tribology in nano-scale and scanning probe microscopy.

Cem Çelebi received his pH.D. in 2009 from Applied Physics Department of Eindhoven University of Technology in the Netherlands. He is currently working as Associate Professor in the Physics Department of IZTECH. He is the principal investigator and group leader of Quantum Device Laboratory at IZTECH. For further information please visit <http://qdl.izte.edu.tr/>